PHYSICS AND CHEMISTRY OF SOLID STATE
V. 25, No. 1 (2024) pp. 26-34
Section: Chemistry

DOI: 10.15330/pcss.25.1.26-34

Vasyl Stefanyk Precarpathian National University

ФІЗИКА І ХІМІЯ ТВЕРДОГО ТІЛА
Т. 25, № 1 (2024) С. 26-34
Хімічні науки

UDK: 544.31:546.22'24'86 ISSN 1729-4428

F.R. Aliyev[1], E.N. Orujlu[1], L.F. Mashadiyeva[2], G.B. Dashdiyeva[3], D.M. Babanly[2,4]

Solid – phase equilibria and thermodynamic properties of the Sb-Te-S system

[1]*Azerbaijan State Oil and Industry University (ASOIU), Azerbaijan, Baku, fariz_ar@hotmail.com*
[2]*Institute of Catalysis and Inorganic Chemistry (ICIC), Azerbaijan, Baku*
[3]*Baku Engineering University (BEU), Azerbaijan, Baku*
[4]*French - Azerbaijani University (UFAZ), Azerbaijan, Baku*

The powder X-ray diffraction (PXRD) analysis and the electromotive force (emf) measurements have been used to investigate the Sb–Te–S system in the Sb_2S_3-Sb_2Te_3-Te-S composition region at 300–450 K temperatures interval. Relative partial molar functions of antimony in alloys have been calculated and obtained data have been used to get self-consistent sets of the standard Gibbs free energy, standard enthalpy, and standard entropy of the Sb_2S_3 and Sb_2Te_2S compounds, as well as the $Sb_2Te_{2,4}S_{0,6}$ and $Sb_2Te_{2,7}S_{0,3}$ solid solutions. The data obtained for Sb_2S_3 have been compared to the ones available in the literature. Thermodynamic functions of the Sb_2Te_2S compound, as well as the $Sb_2Te_{2,4}S_{0,6}$ and $Sb_2Te_{2,7}S_{0,3}$ solid solutions have been determined for the first time.

Keywords: antimony sulfide, antimony telluride, Sb_2Te_2S, tetradymite, EMF measurements, thermodynamic properties.

Received 06 October 2023; Accepted 25 January 2024.

Introduction

The layered tetradymite mineral – Bi_2Te_2S and its analogues $B^V_2Te_2X$ (B^V = Sb, Bi; X= S, Se) have individual functional properties [1-7]. Due to promising electro-physical properties, these compounds have been at the center of consideration of researchers since the middle of the last century. The discovery of a three-dimensional topological insulator (TI) [8-10] which demonstrates special transport properties of electrons has led to increased interest in tetradymite-like layered compounds and doped phases based on them [11-16]. It was observed that solid solutions previously known as thermoelectrics [17-22] demonstrate TI properties [23-25] with various possible applications in quantum computers, medicine, magnetic storage media, security systems, spintronics etc. [26-30].

Thermodynamic properties of compounds and solid solutions are considered their fundamental characteristics and together with phase diagrams they create a pillar for synthesis, crystal growth, doping, optimization etc. of related materials [31,32].

Thermodynamic properties of Sb_2S_3 and Sb_2Te_3 compounds were investigated by different methods and gathered in numerous electronic databases and handbooks [33-36]. However, there is not any published data about thermodynamic study of the Sb_2Te_2S ternary compound.

Phase relations in the Sb_2Te_3-Sb_2S_3 quasi-binary system at first were studied by authors of [37]. According to their results, phase diagram is characterized as of eutectic type without any intermediate compound. However, recently [38] a new tetradymite phase - Sb_2Te_2S located in the Sb_2Te_3-Sb_2S_3 system has been discovered. According to [38], Sb_2Te_2S has a rhombohedral $R\bar{3}$ structure with following lattice constants: a = 10.129(1), c = 23.763(1). In this work, the Sb_2Te_2S compound was not detected in the phase diagram of the Sb_2Te_3-Sb_2S_3 system. Consequently, we have re-investigated the phase diagram of the Sb_2Te_3-Sb_2S_3 system in detail [39]. It was determined that, there is one ternary compound - Sb_2Te_2S in this quasi-binary system melting at 758 K. Refined structural parameters were also reported in [39]:

a = 4.1675 Å, c = 29.483 Å.

Considering above mentioned information, main goal of the present contribution is to investigate solid-state equilibria of the Sb-S-Te ternary system in the Sb_2S_3-Sb_2Te_3-Te-S composition region and determine thermodynamic properties of the chalcogenide phases in the system by means of the emf measurements.

Various modifications of this method are widely used to investigate binary and more complex inorganic compounds [40-46]. During the study of metal chalcogenide phases, it is reasonable to carry out emf measurements in a temperature range below the solidus of corresponding system. For low-temperature measurements, the most relevant electrolytes are glycerol solutions of alkali metal salts [40-44]. Recent studies show that [45, 46], ionic liquids can also be used as a liquid electrolyte in these experiments.

I. Experimental part

For rational planning of experiments, the solid phase equilibria in the Sb_2S_3-Sb_2Te_3-Te-S concentration area of the Sb-Te-S system have been investigated. Considering experimental PXRD results of thermally treated alloys together with the existing information on the phase diagram of the Sb_2S_3-Sb_2Te_3 [39] and boundary binary Sb-S(Te); S-Te systems [47], the schematic phase diagram of the Sb-S-Te ternary system in the Sb_2S_3-Sb_2Te_3-Te-S composition interval was constructed at room temperature. These data suggest that, at room temperature the phase diagram of the Sb_2S_3-Sb_2Te_3-Te-S subsystem should have the form shown in Fig. 1.

In order to determine borders of phase areas in the indicated concentration area, the Sb_2S_3 + Te, Sb_2Te_2S+Te, β (80 mol% Sb_2Te_3) +Te and β (90 mol% Sb_2Te_3) +Te mixtures in the 2:1 weight ratio have been prepared and analysed bv the PXRD method. High purity elemental components have been used for synthesis: Sb (Sigma Aldrich, 99.999%), S (Alpha Aesar, 99.999%) and Te (Sigma Aldrich, 99.999%). The alloys were prepared from presynthesized and identified compounds and high-purity elemental tellurium in quartz ampoules pumped down to ~10^{-2} Pa. After melting at 1000 K, the samples were cooled to 700 K and held there for 500 hours [39, 48].

X-ray powder diffraction patterns were collected on a Bruker D2 PHASER diffracttometer with CuK_α radiation within 2θ=5º-70º range. The powder diffractograms of the obtained equilibrium samples are given in Fig. 2. As can be seen from Fig. 2, all three equilibrated alloys consist of Sb_2S_3 + Te, Sb_2Te_2S+Te, β (80 mol% Sb_2Te_3)+Te two-phase mixtures. Existence of two-phase mixtures along the Sb_2S_3-Sb_2Te_3 system has proved that in the indicated concentration field, all phases are in a direct connode connection with elemental tellurium.

For the experimental study of the Sb-Te-S system by the EMF method, the concentration cells of the type

$$(-)Sb\ (solid)|glycerol + Sb^{3+}|Sb - S - Te(solid)(+) \quad (1)$$

were prepared and their EMF measurements were provided at the 300–450 K temperature range.

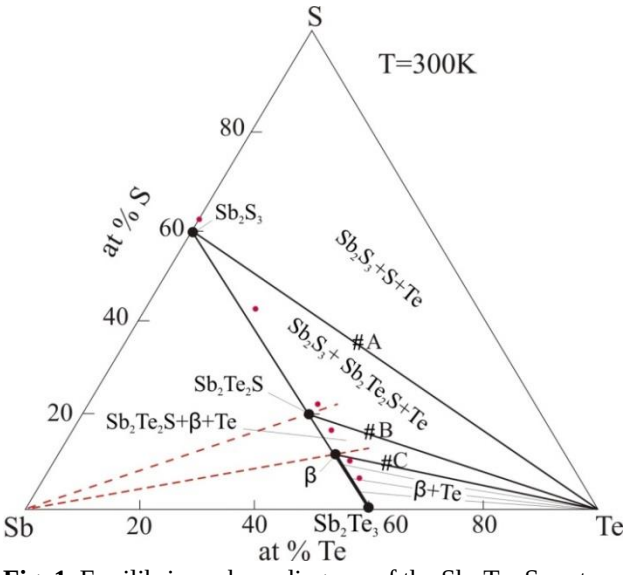

Fig. 1. Equilibrium phase diagram of the Sb–Te–S system in the Sb_2S_3-Sb_2Te_3-Te-S composition region at 300 K. A, B and C represent the composition of the alloys whose X-ray image is shown in Fig. 2.

An elemental antimony was used as the left electrode in the cell of type (1). Compositions of the right electrodes have been chosen based on the solid phase diagram (Fig.1) of the system. As it is obvious from the diagram, the ray lines coming from the Sb corner of the concentration triangle and passing through the stoichiometric composition of the Sb_2Te_2S compound and the boundary composition of the β (80 mol% Sb_2Te_3) solid solution enter the Sb_2S_3 + Sb_2Te_2S + Te and Sb_2Te_2S + β (80 mol% Sb_2Te_3) +Te three-phase fields, respectively. It shows that [40,49], to study thermodynamic properties of these phases, the equilibrium alloys taken from the indicated three-phase fields can be used as right electrodes in the concentration cell of the type (1). Hence, the alloys of the 40, 60, 70, 80 and 90 mol% Sb_2Te_3 composition along the Sb_2S_3 + Sb_2Te_3 system with excess of ~2 wt.% of Te have been synthsized according to the above given methodology. To adapt the state of samples closer to the temperature of EMF measurements, thermal treatment at 700K was followed by holding them at ~400 K for an additional 100 hours.

An electrolyte - glycerol solution of anhydrous KCl (Sigma Aldrich, 99.999%) with an addition of 0.1 wt.% of anhydrous $SbCl_3$ (Merck, 99.999%) have been used as an electrolyte during experiments. Due to the presence of moisture or oxygen in the electrolyte, glycerol was thoroughly dehydrated and degassed at ~450 K under a dynamic vacuum and anhydrous chemically pure salts were used. Preparation of the electrolyte and electrodes, as well as assembly of the electrochemical cell (1) were put into practice as described in [42-44, 49].

Experimental data were collected using the

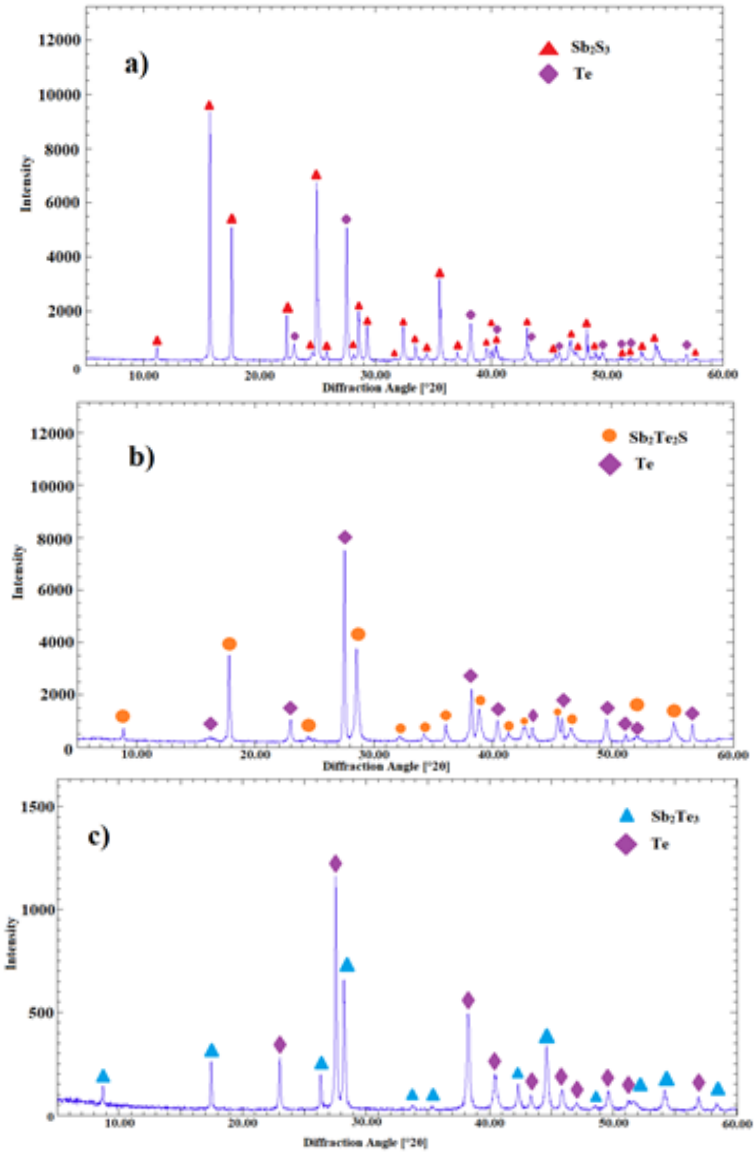

Fig. 2. X-ray powder diffraction patterns of the alloys A, B and C in the Fig.1:alloy A - Sb_2S_3+5Te; alloy B - Sb_2Te_2S+5Te; alloy C - 80%Sb_2Te_3 +5Te.

Keithley 2100 6 1/2 Digital Multimeter. After keeping the cell at ~350 K for 40–60 hours, the first equilibrium values of the potential difference were obtained. Then subsequent measurements were taken every 3-4 h when a particular temperature was established. Repeated measurements at given temperature did not differ from each other by more than 0.2 mV regardless of whether the temperature was increased or decreased.

II. Results and discussions

The emf measurements showed their reproducibility and well agreement with Fig. 2. The E–x diagram (Fig. 3) shows that, the emf is a monotonous function of composition within the homogeneity region of the β-phase. However, it remains constant independent of the overall composition of the electrode alloy in the Sb_2S_3 + Sb_2Te_2S and Sb_2Te_2S + β (80 mol% Sb_2Te_3) two-phase fields on the T-x diagram of the Sb_2S_3-Sb_2Te_3 system. Moreover, the analysis of the temperature dependences of the emf of the alloys in the indicated areas has shown that they are practically linear (Fig. 4). It shows that the compositions of coexisting phases in the given heterogeneous areas in the studied temperature range are constant, and it gives a base for estimations of the partial entropy and enthalpy from values of the temperature coefficients of the emf [49-51]. Given this, collected experimental emf and temperature data were analyzed using least squares method to yield linear equations of the form $E = a + bT$ (2) [49-53]. The calculation procedure for the Sb_2S_3+S+Te phase area has been illustrated in Table 1. Temperature dependencies of the emf data for the Sb_2S_3+Sb_2Te_2S+Te; Sb_2Te_2S+β($Sb_2Te_{2.4}S_{0.6}$) +Te and β ($Sb_2Te_{2.7}S_{0.3}$) +Te phase regions of the Sb_2S_3-Sb_2Te_3-Te-S system are given in the Table 2.

Obtained linear equations of the type (2) are presented in the Table 3 in the form recommended by [40]:

$$E = a + bT \pm t\,[(S_E^2\ /\mathrm{n}) + S_b^2\ (T - \bar{T})^2]^{1/2} \qquad (2)$$

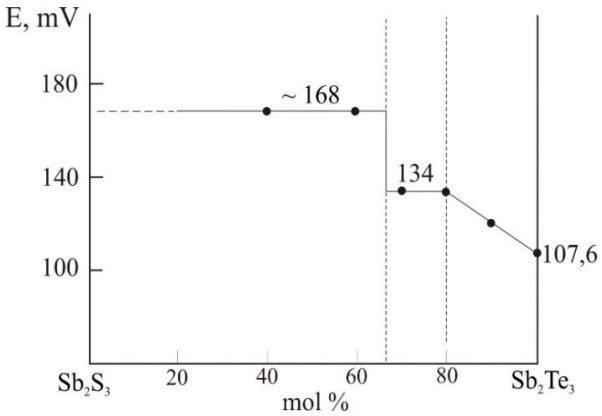

Fig. 3. Relationship between the EMF of concentration chains of type (1) and alloy composition.

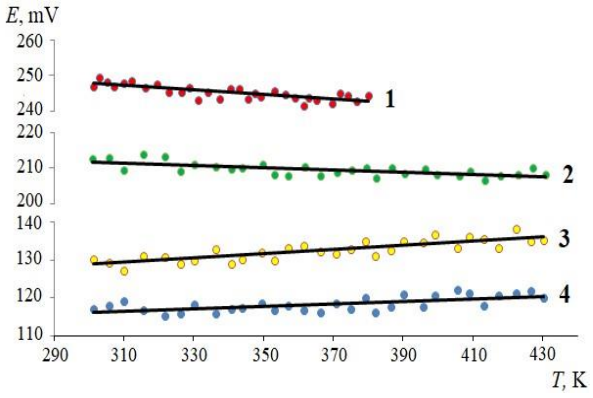

Fig. 4. Temperature dependences of the emf for cells of the type (1) in the Sb–Te–S system. Phase fields: (1) Sb_2S_3+S+Te; (2) Sb_2S_3+Sb_2Te_2S+Te; (3) Sb_2Te_2S+β($Sb_2Te_{2.4}S_{0.6}$)+Te; (4) β ($Sb_2Te_{2.7}S_{0.3}$)+Te.

Table 1.

Computer-processed emf measurement results for a sample from the Sb_2S_3+S+Te phase field of the Sb-Te-S system

T_i, K	E_i, mV	$T_i - \bar{T}$	$E_i(T_i - \bar{T})$	$(T_i - \bar{T})^2$	$\tilde{E}$	$E_i - \tilde{E}$	$(E_i - \tilde{E})^2$
301.2	246.13	-39.04	-9608.09	1523.86	246.86	-0.73	0.53
302.9	248.22	-37.34	-9267.71	1394.03	246.77	1.45	2.09
305.1	247.31	-35.14	-8689.65	1234.59	246.66	0.65	0.42
307	246.27	-33.24	-8185.19	1104.68	246.57	-0.30	0.09
309.8	246.98	-30.44	-7517.25	926.39	246.42	0.56	0.31
312.2	247.44	-28.04	-6937.39	786.05	246.30	1.14	1.29
316.1	245.86	-24.14	-5934.24	582.58	246.11	-0.25	0.06
319.3	246.75	-20.94	-5166.12	438.34	245.94	0.81	0.65
322.8	245.01	-17.44	-4272.16	304.04	245.77	-0.76	0.57
326.4	244.98	-13.84	-3389.71	191.45	245.59	-0.61	0.37
328.6	246.03	-11.64	-2862.97	135.41	245.47	0.56	0.31
331.2	243.15	-9.04	-2197.27	81.66	245.34	-2.19	4.81
333.9	244.89	-6.34	-1551.79	40.15	245.21	-0.32	0.10
337.2	243.35	-3.04	-738.97	9.22	245.04	-1.69	2.86
340.5	245.67	0.26	64.69	0.07	244.87	0.80	0.63
342.8	245.58	2.56	629.50	6.57	244.76	0.82	0.68
345.3	243.42	5.06	1232.52	25.64	244.63	-1.21	1.47
347.4	244.74	7.16	1753.15	51.31	244.53	0.21	0.05
349.1	243.99	8.86	2162.56	78.56	244.44	-0.45	0.20
353	245.12	12.76	3128.55	162.90	244.24	0.88	0.77
356.1	244.53	15.86	3879.06	251.65	244.09	0.44	0.20
358.9	243.82	18.66	4550.49	348.32	243.94	-0.12	0.02
361.3	242.01	21.06	5097.54	443.66	243.82	-1.81	3.29
362.7	243.75	22.46	5475.44	504.60	243.75	0.00	0.00
365.1	243.14	24.86	6045.27	618.19	243.63	-0.49	0.24
369.4	242.43	29.16	7070.07	850.50	243.41	-0.98	0.97
371.6	244.74	31.36	7675.86	983.66	243.30	1.44	2.07
373.8	244.17	33.56	8195.16	1126.50	243.19	0.98	0.96
376.5	242.92	36.26	8809.09	1315.03	243.06	-0.14	0.02
379.9	244.21	39.66	9686.18	1573.18	242.88	1.33	1.76
$\bar{T}$ =340.236	$\bar{E}$ =244.887		$\sum$ =-863.37	$\sum$ =17092.79			$\sum$ =27.77

here *a* and *b* are constant coefficients, n is the number of data points (E and T), t is Student's t, is the variance of an individual emf measurement, and is the variance of the coefficient b. For a number of data points n = 30 and a 95% confidence interval, we have $t \leq 2$.

The partial molar functions of antimony in the indicated areas had been calculated from these linear equations (Table 3) using the following thermodynamic relations:

$$\Delta\bar{G}_{Sb} = -zFE \qquad (3)$$

Table 2.

Experimental data for temperature ($\mathbf{T_i}$,) and emf ($\mathbf{E_i}$) for the Sb_2S_3+Sb_2Te_2S+Te (I); Sb_2Te_2S+β($Sb_2Te_{2.4}S_{0.6}$) +Te (II); and β ($Sb_2Te_{2.7}S_{0.3}$)+Te (III) phase areas of the Sb-Te-S system

	Ei, mV		
	Phase area		
	I	**II**	**III**
301.2	212.45	130.15	117.21
305.9	212.72	129.22	118.09
310.1	209.38	127.28	119.28
315.6	213.74	131.14	116.94
321.8	213.01	130.91	115.36
326.2	208.94	129.04	116.04
330.1	210.86	129.86	118.26
336.3	210.15	132.95	115.95
340.8	209.71	129.11	117.11
344	209.98	130.28	117.48
349.6	211.03	132.03	118.73
353.2	208.15	129.85	116.85
357.1	207.89	133.29	118.09
361.6	210.35	133.85	116.85
366.3	207.67	132.17	116.17
370.9	208.58	131.68	118.68
375.1	209.42	133.02	117.02
379.4	209.94	134.94	119.94
382.1	207.18	131.18	116.18
386.5	210.12	132.72	117.82
390.1	208.53	135.03	121.03
395.9	209.82	134.82	117.82
399.3	208.01	136.61	120.61
405.7	207.75	133.15	122.15
408.9	208.94	136.24	121.24
413.1	206.43	135.43	118.08
417.3	207.74	133.24	120.74
422.5	208.17	138.17	121.17
426.7	209.92	134.92	121.92
430.2	208.11	135.13	120.13

$$\Delta\bar{S}_{Sb} = zF\left(\frac{\partial E}{\partial T}\right)_P = zFb \qquad (4)$$

$$\overline{\Delta H}_{Sb} = -zF\left[E - T\left(\frac{\partial E}{\partial T}\right)_P\right] = -zFa \qquad (5)$$

Obtained relative partial molar functions of antimony in the alloys are presented in Table 4.

Sb_2S_3 is the only compound in the Sb-S binary system. Therefore, the partial molar functions of antimony in the Sb_2S_3 + S +Te phase field correspond to the

$$Sb(s) + 1.5 \cdot S(s) = 0.5 \cdot Sb_2S_3(s) \qquad (6)$$

potential-generating reaction. This reaction is like the reaction of formation of Sb_2S_3 compound from its elemental components. Therefore, the corresponding partial molar functions of antimony are thermodynamic functions of Sb_2S_3 formation for 1 g/at of antimony.

The standard integral thermodynamic functions of formation (Z ≡ G, H) and standard entropy of Sb_2S_3 were calculated using the following relations:

$$\Delta_f Z^0(Sb_2S_3) = 2\Delta\overline{Z_{Sb}} \qquad (7)$$

$$S^0(Sb_2S_3) = 2\Delta\overline{S_{Sb}} + 2\,S^0(Sb) + 3\,S^0(S) \qquad (8)$$

Taking into account the constancy of the compositions of the coexisting phases in the three-phase regions Sb_2S_3+Sb_2Te_2S+Te and Sb_2Te_2S+β($Sb_2Te_{2.4}S_{0.6}$) +Te, the standard integral thermodynamic properties of the Sb_2Te_2S compound and the limiting composition of beta-solid solutions ($Sb_2Te_{2.4}S_{0.6}$) were calculated by the method of potential-forming reactions [40,49]. According to Fig.2, the partial molar functions of Sb in the above three-phase regions are thermodynamic functions of the following potential-forming reactions:

$$Sb + 0.25\,Sb_2S_3 + 1{,}5\,Te = 0.75\,Sb_2Te_2S \qquad (9)$$

$$Sb + 0.75\,Sb_2Te_2S + 1.5\,Te = 1.25\,Sb_2Te_{2,4}S_{0.6} \qquad (10)$$

According to these reactions, the standard thermodynamic functions for the formation of ternary phases were calculated from

$$\Delta_f Z^0(Sb_2Te_2S) = 1\tfrac{1}{3}\overline{\Delta Z}_{Sb} + \tfrac{1}{3}\Delta_f Z^0(Sb_2S_3) \qquad (11)$$

$$\Delta_f Z^0(Sb_2Te_{2.4}S_{0.6}) = 0.8\overline{\Delta Z}_{Sb} + 0.6\Delta_f Z^0(Sb_2Te_2S) \qquad (12)$$

relations, and their standard entropies - using following equations:

$$S^0(Sb_2Te_2S) = 1\tfrac{1}{3}\overline{\Delta S}_{Sb} + 1\tfrac{1}{3}S^0(Sb) + 2S^0(Te) + \tfrac{1}{3}S^0(Sb_2S_3) \qquad (13)$$

$$S^0\left(Sb_2Te_{2,4}S_{0,6}\right) = 0.8\overline{\Delta S}_{Sb} + 0.8S^0(Sb) + 1.2S^0(Te) + 0.6S^0(Sb_2Te_2S) \qquad (14)$$

The calculation of the standard thermodynamic functions of the formation of β-solid solutions of the $Sb_2Te_{2,7}S_{0,3}$ composition was carried out by graphical integration of the Gibbs-Duhem equation along the Sb_2Te_3-Sb_2S_3 section according to the well-known method [40,49].

Obtained results are presented in Table 4. Uncertainties were evaluated by the error accumulation method. In calculating the integral thermodynamic functions, we used, in addition to the data in Table 4, the standard entropies of antimony (45.7 ± 0.6 J/(mol K)), sulfur (31.9 ± 0.2 J/(mol K)), and tellurium (49.5 ± 0.2 J/(mol K)) [35]. Table 5 also contains published data on the thermodynamic functions of Sb_2S_3 and Sb_2Te_3. Our results for the Sb_2S_3 differ very little from the data recommended by [33,34]. The thermodynamic

Table 3.

Equations of the temperature-dependent emf of cells of the type (1) in some phase fields of the Sb_2S_3-Sb_2Te_3-Te-S system

Phase field	$E = a \pm bT \pm 2S_E\,(T)$
Sb_2S_3+S+Te	$267.07 - 0.0505T \pm 2\left[\frac{0.93}{30} + 5.4 \cdot 10^{-5}\,(T - 340.2)^{\,2}\right]^{1/2}$
Sb_2S_3+Sb_2Te_2S+Te	$180.96 - 0.0312T \pm 2\left[\frac{1.68}{30} + 3.8 \cdot 10^{-5}\,(T - 367.5)^{\,2}\right]^{1/2}$
Sb_2Te_2S+β($Sb_2Te_{2.4}S_{0.6}$)+Te	$112.0 + 0.056T \pm 2\left[\frac{2.07}{30} + 2.1 \cdot 10^{-5}\,(T - 367.5)^{\,2}\right]^{1/2}$
β ($Sb_2Te_{2.7}S_{0.3}$)+Te	$106.3 + 0.033T \pm 2\left[\frac{2.09}{30} + 4.8 \cdot 10^{-5}\,(T - 367.5)^{\,2}\right]^{1/2}$

Table 4.

Partial molar functions of Sb in alloys of the Sb_2S_3-Sb_2Te_3-Te-S system (298 K)

Phase field	$-\Delta\bar{G}_{Sb}$	$-\Delta\bar{H}_{Sb}$	$-\Delta\bar{S}_{Sb}$
	kJ·mole^{-1}		*J·mole^{-1}·K^{-1}*
Sb_2S_3+S+Te	71,50 ± 0,09	75,86 ± 0,72	-14,62±2,13
Sb_2S_3+Sb_2Te_2S+Te	49,69 ± 0,15	52,38 ± 0,66	-9,04±1,80
Sb_2Te_2S+β($Sb_2Te_{2.4}S_{0.6}$)+Te	37,25 ± 0,15	32,42 ± 0,75	16,21±2,02
β ($Sb_2Te_{2.7}S_{0.3}$)+Te	33,62 ± 0,15	30,77 ± 0,75	9,56±2,02

Table 5.

Standard integral thermodynamic functions of the phases in the Sb–S–Te system

Phase field	$-\Delta\bar{G}_{Sb}$	$-\Delta\bar{H}_{Sb}$	$\Delta_f S^0$	S^0	***Reference, method, temperature***
	kJ·mole^{-1}		*J·mole^{-1}·K^{-1}*		
Sb_2S_3	143,0±0,2	151,7±1,5	-29,2±4,3	157,7±5,9	This work, EMF
	140.29	141.80	-	182.17	[33] recommended
	140.5 ± 4.2	141.8 ± 4.1	-	182.0 ± 3.3	[34]
	156.08	157.74	-	181.6 ± 4.2	[35]
Sb_2Te_2S	113,9±0,3	120,4±1,4	-21,9±3,7	200,2±5,5	This work, EMF
β($Sb_2Te_{2,4}S_{0,6}$)	98,1±0,4	98,2±1,1	-0,3±3,8	228,9±5,7	This work, EMF
β($Sb_2Te_{2,7}S_{0,3}$)	82,7±0,4	79,9±1,3	9,4±4,0	243,8±6,1	This work, EMF
Sb_2Te_3	64,46±0,18	59,06±0,98	8,0±2,8	247,5±4,4	[36] EMF, 300-450 K

functions of tetradymite (Sb_2Te_2S) and a tetradymite-based solid solution with the $Sb_2Te_{2,4}S_{0,6}$ and $Sb_2Te_{2.7}S_{0.3}$ compositions have been estimated by us for the first time (Table 5).

Conclusion

The Sb–S–Te system has been studied using PXRD and emf measurements in the Sb_2S_3-Sb_2Te_3-Te-S composition region at the 300–450 K temperatures range. The relative partial molar functions of antimony in alloys have been calculated. Taking into consideration the solid phase diagram of the Sb_2S_3-Sb_2Te_3-Te-S subsystem, the potential-generating reactions which have then been used to calculate the standard Gibbs free energy, standard enthalpy, standard entropy of the Sb_2S_3, Sb_2Te_2S compounds, as well as $Sb_2Te_{2,4}S_{0,6}$ and $Sb_2Te_{2,7}S_{0,3}$ solid solutions were determined. The present results for Sb_2S_3 compound supplement and improve thermodynamic data available in the literature, whereas the thermodynamic functions of the ternary phases have been determined for the first time.

Aliyev F.R. – ***PhD*** student on Chemistry;
Orujlu E.N. – PhD on Chemistry;
Mashadiyeva L.F. –Associate Professor, Senior Researcher;
Dashdiyeva G.B. – PhD on Chemistry, Lecturer;
Babanly D.M. – Dr. of Sciences on Chemistry, Lecturer, Senior Researcher.

[1] J. Sung-Jae, R. Byungki, S. Ji-Hee, J. Lee, B. Min, B. Kim, *Highly anisotropic thermoelectric transport properties responsible for enhanced thermoelectric performance in the hot-deformed tetradymite Bi2Te2S*, Journal of Alloys and Compounds. 783, 448 (2019); https://doi.org/10.1016/j.jallcom.2018.12.340.
[2] A. Asif, H. Naqib, *A DFT based first-principles investigation of optoelectronic and structural properties of Bi_2Te_2Se,* Physica Scripta. 96(4), 045810 (2021); https://doi.org/ 10.1088/1402-4896/abe2d2.
[3] L. Peng, K. Pei, et al., *Ultrathin 2D ternary Bi2Te2Se flakes for fast-response photodetectors with gate-tunable* responsivity, Sci. China-Mater. 64, 3017 (2021); https://doi.org/10.1007/s40843-021-1695-x.

[4] X. Bin, Q. Xia, et al., *High figure of merit of monolayer Sb2Te2Se of ultra low lattice thermal conductivity*, Computational Materials Science. 177, 109588 (2020); https://doi.org/10.1016/j.commatsci.2020.109588.
[5] R. Samrat, S. Manna, et al., *Photothermal Control of Helicity-Dependent Current in Epitaxial Sb_2Te_2Se Topological Insulator Thin-Films at Ambient Temperature*, ACS Applied Materials & Interfaces. 14 (7), 9909 (2022); https://doi.org/10.1021/acsami.1c24461.
[6] J. Reimann, K. Kuroda, et al., *Spectroscopy and dynamics of unoccupied electronic states of the topological insulators Sb2Te3 and Sb2Te2S*, Physical Review B., 90(8), 081106 (2014); https://journals.aps.org/prb/abstract/10.1103/PhysRevB.91.039903.
[7] M. Kanagaraj, P. Amit, et al., *Structural, magnetotransport and Hall coefficient studies in ternary Bi2Te2Se, Sb2Te2Se and Bi2Te2S tetradymite topological insulating compounds*, Journal of Alloys and Compounds. 794, 195 (2019); https://doi.org/10.1016/j.jallcom.2019.04.226.
[8] M. Joel., *The birth of topological insulators*, Nature. 464, 7286 (2010); https://www.nature.com/articles/nature08916.
[9] H. Zahid, J. Moore, E. Annu., *Three-Dimensional Topological Insulators*, Rev. Condens. Matter Phys., 2(1), 55 (2011); https://doi.org/10.1146/annurev-conmatphys-062910-140432.
[10] R. Stephan, *Interacting topological insulators: a review*, Reports on Progress in Physics. 81(11), 116501 (2018); https://iopscience.iop.org/article/10.1088/1361-6633/aad6a6/meta.
[11] E. V. Chulkov, Z. S. Aliev, A. V. Shevelkov, I. R. Amiraslanov, *Phase diagrams in materials science of topological insulators based on metal chalcogenides*, Russian Journal of Inorganic Chemistry 62, 1703 (2017); https://doi.org/10.1134/S0036023617130034.
[12] E. Orujlu, Z. Aliev, M. Babanly, *The phase diagram of the MnTe–SnTe–Sb2Te3 ternary system and synthesis of the iso- and aliovalent cation-substituted solid solutions*, Calphad., 76, 102398 (2022); https://doi.org/10.1016/j.calphad.2022.102398.
[13] A. Shikin, A. Estyunin, I. Klimovskikh, et al., *Nature of the Dirac gap modulation and surface magnetic interaction in axion antiferromagnetic topological insulator MnBi2Te4*, Scientific Reports. 10(1), 13226 (2020); https://doi.org/10.1038/s41598-020-70089-9.
[14] I. Klimovskikh, O. Mikhail, et al., *Tunable 3D/2D magnetism in the (MnBi2Te4)(Bi2Te3)m topological insulators family*, npj Quantum Materials. 5(1), 54 (2020); https://doi.org/10.1038/s41535-020-00255-9.
[15] T. Alakbarova, E. Orujlu, D. Babanly, *Solid-phase equilibria in the GeBi2Te4-Bi2Te3-Te system and thermodynamic properties of compounds of the GeTe·mBi2Te3 homologous series*, Physics and Chemistry of Solid State. 23(1), 25 (2022); https://doi.org/10.15330/pcss.23.1.25-33.
[16] D. Pacilè, S. Eremeev, M. Caputo, et al. *Deep Insight Into the Electronic Structure of Ternary Topological Insulators: A Comparative Study of $PbBi_4Te_7$ and $PbBi_6Te_{10}$,* Physica status solidi (RRL)–Rapid Research Letters, 612(12), 1800341 (2018); https://doi.org/10.1002/pssr.201800341.
[17] L. Shelimova, G. Karpinskii, P. Konstantinov, et al, *Crystal Structures and Thermoelectric Properties of Layered Compounds in the ATe–Bi2Te3(A = Ge, Sn, Pb) Systems*, Inorganic Materials. 40, 451 (2004); https://doi.org/10.1023/B:INMA.0000027590.43038.a8.
[18] S. Zemskov, E. Shelimova, P. Konstantinov, et al., *Thermoelectric materials based on layered chalcogenides* of bismuth and lead, Inorganic Materials: Applied Research, 3, 61 (2012); https://doi.org/10.1134/S2075113312010133;
[19] B. Xu, L. Song, G. Peng, et al., Thermoelectric performance of monolayer Bi2Te2Se of ultra low lattice thermal conductivity, Physics Letters A, 383(28), 125864 (2019); https://doi.org/10.1016/j.physleta.2019.125864.
[20] S. Yixuan, C. Sturm, H. Kleinke. *Chalcogenides as thermoelectric materials*, Journal of Solid State Chemistry. 270, 273 (2019); https://doi.org/10.1016/j.jssc.2018.10.049.
[21] C. Ying, et al., *Renormalized thermoelectric figure of merit in a band-convergent Sb_2Te_2Se monolayer: full electron–phonon interactions and selection rules*, Journal of Materials Chemistry A., 9(29), 16108 (2021); https://doi.org/10.1039/D1TA02107A.
[22] R. Medha, D. Jana, D. Banerjee, *General strategies to improve thermoelectric performance with an emphasis on tin and germanium chalcogenides as thermoelectric materials*, Journal of Materials Chemistry A 10(13), 6872 (2022); https://doi.org/10.1039/D1TA10421G.
[23] X. Ning, Y. Xu, *Topological insulators for thermoelectrics*, J. Zhu. npj Quantum Materials 2(1), 51 (2017); https://doi.org/10.1038/s41535-017-0054-3.
[24] Y. Ivanov, A. Burkov, D. Pshenay-Severin., *Thermoelectric Properties of Topological Insulators*, Physica status solidi (b) 255(7), 1800020 (2018); https://doi.org/10.1002/pssb.201800020.
[25] H. Joseph, R. Cava, N. Samarth, *Tetradymites as thermoelectrics and topological insulators*, Nature Reviews Materials, 2(10), 17049 (2017); https://doi.org/10.1038/natrevmats.2017.49.
[26] Y. Ming, H. Zhou, J. Wang, *Topological insulators photodetectors: Preparation, advances and application challenges*, Materials Today Communications. 33, 104190 (2022); https://doi.org/10.1016/j.mtcomm.2022.104190.
[27] H. Mengyun, H. Sun, Q.L. He., *Topological insulator: Spintronics and quantum computations*, Frontiers of Physics 14. 43401 (2019); https://doi.org/10.1007/s11467-019-0893-4.
[28] T. Wenchao, W. Yu, et al., *The Property, Preparation and Application of Topological Insulators: A Review*, Materials 10(7), 814 (2017); https://doi.org/10.3390/ma10070814.

[29] L. Viti, D. Coquillat, A. Politano, K.A. Kokh, Z. Aliev, M. Babanly, E. Oleg, et al., *Plasma-Wave Terahertz Detection Mediated by Topological Insulators Surface States*, Nano Lett. 16, 80, (2016); https://doi.org/10.1021/acs.nanolett.5b02901.
[30] Y. Chenxi, S. Jiang, et al., Device Applications of Synthetic Topological Insulator Nanostructures, Electronics. 7(10), 225 (2018); https://doi.org/10.3390/electronics7100225.
[31] G. F Voronin, I. Y. Gerasimov, *The role of chemical thermodynamics in the development of semiconductor materials science*, Thermodynamics and Semiconductor Material Science. Moscow: MIET Publ. 3, (1980).
[32] M.B. Babanly, L.F. Mashadiyeva, D.M. Babanly, S.Z. Imamaliyeva, D.B. Tagiev, Yu.A. Yusibov., *Some Issues of Complex Studies of Phase Equilibria and Thermodynamic Properties in Ternary Chalcogenide Systems Involving Emf Measurements (Review)*, Russ. J. Inorg. Chem, 64(13), 1649 (2019); https://doi.org/10.1134/S0036023619130035.
[33] I. Barin. Thermochemical Data of Pure Substances, 3rd edition Wiley-VCH, (2008).
[34] G.K. Johnson, G.N. Papatheodorou, C.E. Johnson., *The enthalpies of formation of SbF5(l) and Sb2S3(c) and the high-temperature thermodynamic functions of Sb2S3(c) and Sb2S3(l),* J. Chem. Thermodyn. 13(8), 745 (1981); https://doi.org/10.1016/0021-9614(81)90063-X.
[35] V.S. Iorish, V.S. Yungman. (Eds.) Thermal constants of substances: Database. Version 2 (2006) (http://www.chem.msu.ru/cgi-bin/tkv.pl?show=welcome.html/welcome.html.)
[36] F. Aliyev, E. Orujlu, D. Babanly., *Thermodynamic Properties of the Sb2Te3 compound*, Azerbaijan Chemical Journal. 4, 53 (2021); doi.org/10.32737/0005-2531-2021-4-53-59.
[37] Y. Jafarov, M. Babanly, et al., *Study of the 3Tl2S + Sb2Te3 ↔ 3Tl2Te + Sb2S3 reciprocal system*, Journal of alloys and compounds. 582, 659 (2014); https://doi.org/10.1016/j.jallcom.2013.07.141.
[38] D. Grauer, et al., Thermoelectric properties of the tetradymite-type Bi2Te2S–Sb2Te2S solid solution, Materials Research Bulletin., 44(9), 1926 (2009); https://doi.org/10.1016/j.materresbull.2009.05.002.
[39] F. Aliyev, E. Orujlu, D. Babanly, et al., *An update phase diagram of the Sb2Te3-Sb2S3 system*, Jomard publishing. New Materials, Compounds and Applications. 7(2), 76 (2023); http://jomardpublishing.com/UploadFiles/Files/journals/NMCA/v7n2/Aliyev_et_al.pdf.
[40] A.G. Morachevsky, G.F. Voronin, V.A. Geyderich, I.B. Kutsenok, *Electrochemical methods of investigation in thermodynamics of metal systems*. Akademkniga Publ, Moscow, (2003).
[41] V. Vassiliev, W. Gong. *Electrochemical Cells with the Liquid Electrolyte in the Study of Semiconductor, Metallic and Oxide Systems*, Electrochemical Cells–New Advances in Fundamental Researches and Applications. Ed. Yan Shao, IntechOpen. 71 (2012); https://doi.org/10.5772/39007.
[42] D. Babanly, G. Veliyeva, S. Imamaliyeva, M. Babanly. *Thermodynamic functions of arsenic selenides*, Russian Journal of Physical Chemistry A. 91, 1170 (2017); https://doi.org/10.1134/S0036024417070044.
[43] S. Imamaliyeva, D. Babanly, et al., *Thermodynamic Properties of Tl9GdTe6 and TlGdTe2*, Russian Journal of Physical Chemistry A. 92, 2111 (2018); https://doi.org/10.1134/S0036024418110158.
[44] S. Imamaliyeva, I. Mehduyeva, et al., *Thermodynamic investigations of the erbium tellurides by EMF method,* Physics and chemistry of solid state. 21(2), 312 (2020); https://doi.org/10.15330/pcss.21.2.312-318.
[45] Z.S. Aliev, S.S. Musayeva, S.Z. Imamaliyeva, M.B. Babanly, *Thermodynamic study of antimony chalcoiodides by EMF method with an ionic liquid,* J. Therm. Anal. Calorim. 133(2), 1115 (2018); https://doi.org/10.1007/s10973-017-6812-4.
[46] S.Z. Imamaliyeva, S.S. Musayeva, D.M. Babanly, Y.I. Jafarov, D.B. Tagiyev, M.B. Babanly, *Determination of the thermodynamic functions of bismuth chalcoiodides by EMF method with morpholinium formate as electrolyte,* Thermochimica Acta 679, 178319 (2019); https://doi.org/10.1016/j.tca.2019.178319.
[47] T.B. Massalski, J. L. Murray Bennett, *Binary alloy phase diagrams Materials park,* ASM International, Materials Park, OH, USA. 12, (1990).
[48] F.Aliyev, D. Babanly, et. al, *Layered High-Entropy Alloys Based on Antimony and Bismuth Chalcogenides*, Nova Science Publishers Properties and Uses of Antimony. 73 (2022); https://doi.org/ 10.52305/BMLN5323)
[49] M.B. Babanly, A. Yusibov, Electrochemical Methods in Thermodynamics of Inorganic Systems. (Elm, Baku, 2011).
[50] E.Ahmadov, D. Babanly, S. Imamaliyeva, et al., *Thermodynamic Properties of the Chalcogenide Phases in the Bi–Te–S System,* Inorganicnic Materials. 57, 227 (2021); https://doi.org/10.1134/S0020168521030018.
[51] M.Babanly, A.Kuliyev, Mathematical Problems in Chemical Thermodynamics, Novosibirsk, Nauka, Siberian Section. 192 (1985)
[52] K. Derffel. Statistics in Analytical Chemistry. Mir; Moscow, Russia. 268 (1994).
[53] A.N.Kornilov, L.B.Stepina, V.A. Sokolov, *Recommendations on compact representation of experi mental data in reports on thermochemical and thermo dynamic studies,* Zh. Fiz. Khim. 46(11), 2974 (1972).

Ф.Р. Алієв[1], Е.Н. Оруйлу[1], Л.Ф. Машадієва[2], Г.Б. Дашдієва[3], Д.М. Бабанли[2,4]

Твердофазні рівноваги та термодинамічні властивості системи Sb-Te-S

[1]Азербайджанський державний університет нафти та промисловості (ASOIU), Азербайджан, Баку,
fariz_ar@hotmail.com
[2]Інститут каталізу та неорганічної хімії (ICIC), Азербайджан, Баку,
[3]Бакинський інженерний університет (BEU), Азербайджан, Баку,
[4]Франко - Азербайджанський університет (UFAZ), Азербайджан, Баку

Для дослідження системи Sb–Te–S в області складу Sb_2S_3-Sb_2Te_3-Te-S в інтервалі температур 300–450 K використано порошковий рентгенівський аналіз (PXRD), а також вимірювання електрорушійної сили (EPC). Розраховано відносні парціальні молярні функції сурми в сплавах та відповідні дані використано для отримання самоузгоджених наборів стандартної вільної енергії Гіббса, стандартної ентальпії та стандартної ентропії сполук Sb_2S_3 і Sb_2Te_2S, а також твердих розчинів $Sb_2Te_{2,4}S_{0,6}$ та $Sb_2Te_{2,7}S_{0,3}$. Дані, отримані для Sb_2S_3, порівнювали із наявними в літературі. Вперше визначено термодинамічні функції сполуки Sb_2Te_2S, а також твердих розчинів $Sb_2Te_{2,4}S_{0,6}$ та $Sb_2Te_{2,7}S_{0,3}$.

Ключові слова: сульфід сурми, телурид сурми, Sb_2Te_2S, тетрадиміт, вимірювання EPC, термодинамічні властивості.